RESEARCH ON CORROSION DEGRADATION PROCESS OF SOME THERMAL POWER PLANTS STEAM BOILER PIPES

Cătălin Ştefan GRĂDINARU[1], George COMAN[1*], Sorin CIUCĂ[1], Mirela Gabriela SOHACIU[1], Andrei Constantin BERBECARU[1], Andrei GRECU[1*], Ruxandra Elena DUMITRESCU[1], Ioana Arina GHERGHESCU[1], Cristian PREDESCU[1]

The paper presents the typical corrosion degradation process of some steam boiler pipes, after operating for long periods of time at high temperatures. The oxidizing environment (water vapor, atmospheric oxygen or salts of oxyacids frequently existing in water) favors this type of corrosion, which is very characteristic for common ferrous alloys (OLT45). The mixed iron oxides film that is formed (FeO-$Fe_2O_3 \rightarrow Fe_3O_4$) is very porous, weakly adherent and does not provide any protection to the metallic material.

Keywords: degradation, corrosion, steam boiler pipe

1. Introduction

The present research aimed to establish the phenomena taking place in the degradation process of a steam boiler pipe material after a long operating time. The analyzed pipes were operating for over 200,000 hours. Long term overheating is reported to induce significant problems [1], leading to more and more damages, affecting the activity and integrity of the entire energy plant. Concerns are related with a potential danger to health and life of the personnel servicing the installations and equipment.

2. Materials and investigations

Samples were taken from four pipes from a steam boiler. The following investigation tests were performed:
- determination of the chemical composition by optical emission spectrometry, using the LECO GDS 500A spectrometer;
- macroscopic analysis of the affected surfaces;
- Vickers hardness performed on universal static hardness testing machine BUEHLER - WILSON, REICHERTER UH 250;

[1] Materials Science and Engineering Faculty, Politehnica University of Bucharest, 313 Splaiul Independenței, 060042 Bucharest, Romania,
[*]Cooresponding authors e-mail: george.coman@upb.ro, andrei.grecu2611@upb.ro

- the Vickers in-situ hardness measurements were performed using the General Electric - Krautkramer MIC 20 portable hardness tester;
- optical microscopy metallographic analyses were performed on an OLYMPUS BX 51 M microscope;
- tensile tests were performed using Instron 8802 universal tensile testing machine.

3. Results and Discussion

3.1. Samples chemical composition analyses

The samples chemical compositions determined by optical emission spectrometry are shown in Table 1.

Table 1

Samples chemical compositions

Element /Sample	C %	Mn %	Si %	S %	P %	Cu %	Al %	Cr %	Ni %
10	0.251	0.481	0.254	0.025	0.016	0.151	0.013	0.197	0.169
11	0.240	0.416	0.258	0.022	0.010	0.033	0.007	0.042	0.024
12	0.217	0.418	0.258	0.021	0.010	0.033	0.006	0.041	0.023
13	0.247	0.500	0.272	0.023	0.014	0.116	0.022	0.159	0.197

The compositional data for all samples fall into the steel's grade OLT45, a mark frequently used to make pipes exposed to moderate temperatures and pressures. The new equivalent steel grade used nowadays is E275 (EN 10297). Other steel grades may be chosen [2].

3.2. Macroscopic analysis of the affected surfaces

The four macroscopically investigated pipes showed degradation surfaces typical for dry corrosion or oxidation, which appeared after long periods of operating at higher temperatures than the prescripted ones [3 - 6]. The oxidizing working environment (water vapor, atmospheric oxygen or salts of oxyacids frequently existing in water) favors this type of corrosion, typical for common ferrous alloys, as is the case of the investigated pipes steels (OLT45) samples. The film of mixed iron oxides that is formed ($FeO\text{-}Fe_2O_3 \rightarrow Fe_3O_4$) is very porous, of weak adherence, and it does not provide any protection to the metallic material. Other researchers reported similar phenomena [7 - 10]. Taking place at high temperatures, diffusion phenomena are deciding these oxides formation kinetics: the higher the temperature and the longer the duration, the more intense their growth rate.

Fig. 1. Macroscopic overview of boiler pipes damaged in operation

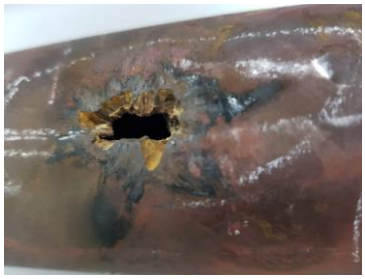

a

b

Fig. 2. Macroscopic image of damaged pipe 11 (a), detail of the sample inner surface (b)

a

b

Fig. 3. Macroscopic image of damaged pipe 12 (a), detail of the sample front side (b)


a


b

Fig. 4. Macroscopic image of damaged pipe 13 (a), detail of the sample right side (b)

Figures 1 – 4 show areas of typical degradation by oxidation: the regions surrounding the perforations are reddish-brick, specific color of the iron (II, III) oxide Fe_3O_4. The corroded area has a "stepped" surface, a specific detail of intercrystalline corrosion, this type of corrosion being commonly found in oxidation phenomena. Moreover, the areas surrounding the corroded regions have longitudinal streaks where the metallic material exfoliates. They are denser the more intense the oxidation phenomena were. The most relevant example is the case of pipe 13, Figure 4a, which is even deformed in the corroded area, where one can see deep streaks that mark the delamination of the metallic material, the corrosion advancing in an intercrystalline manner.

Observing the position of the pipe 13 in the boiler architecture (Fig. 1) one may see that it comes in almost direct contact with the burners flame, which explains the very high oxidation kinetics.

Cross section analysis of pipe 11 (Fig. 2b) supports the statement that the pipes are strongly degraded by oxidation. Thus, inside (on the pipe inner walls) the corrosion area shows a very rough surface, with a reddish-brown shade, typical for FeO oxides. The oxygenated salts existing in the circulating water contributed also to the oxidation phenomena, which, amplified by temperature, led to the advanced chemical corrosion.

The results of the macroscopic analysis highlighted the typical degradation surfaces by corrosion (oxidation) after a long operating time, even above the lifespan of some OLT 45 pipe-type subassemblies, at a temperature that could locally exceed the incandescent threshold of steel (540°C), although according to the operating parameters of the boiler, the circulating water vapour shouldn’t have reach this temperature.

3.3. Hardness tests

Vickers hardness measurements were performed both on samples taken from the boiler and on undamaged pipes found in the vicinity of the replaced ones. Table 2 shows in – situ Vickers hardness values measured in the damaged area of the installation. Five determinations were performed on each sample. The location of the hardness tests performed near the damaged area can be seen in Figure 5.

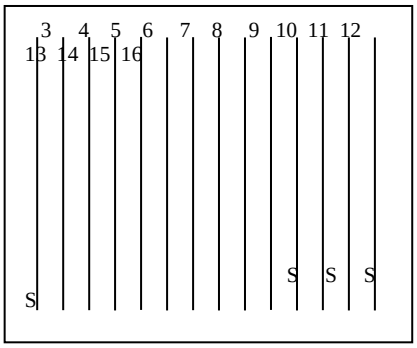

Fig. 5. Schematic representation of the in-situ hardness tested pipes.

Table 2

***In-situ* measurements of HV5 Vickers hardness**

No.	Sample number	HV5 hardness values	Average HV5 value
1	3	165, 167, 170, 162, 160	165
2	4	140, 147, 145, 150, 142	145
3	5	211, 203, 211, 210, 210	209
4	6	201, 197, 195, 188, 190	194
5	7	203, 200, 194, 199, 205	200
6	8	159, 159, 157, 163, 151	158
7	9	154, 157, 158, 162, 158	158
8	10	153, 150, 149, 142, 144	148
9	11	137, 136, 137, 139, 131	136
10	12	125, 126, 125, 129, 124	126
11	13	128, 121, 134, 128, 123	127
12	14	156, 157, 152, 157, 149	154
13	15	158, 141, 143, 149, 150	148
14	16	145, 144, 143, 147, 138	143

The hardness HV5 values found on the pipe samples taken from the damaged sections are:

Table 3

Laboratory HV5 hardness values of the four samples

No.	Sample number	HV5 hardness values	Average HV5 value
1	10	134, 135, 136, 136, 137	136
2	11	129, 134, 136, 139, 117	131
3	12	121, 116, 112, 114, 125	118
4	13	122, 135, 118, 125, 121	124

Hardness values mainly fall into the range of values achievable by OLT45 steel. Slightly lower values than the limit threshold are sometimes recorded, not necessarily related to a loss of pipes steel mechanical strength over time, at least according to the hardness figures.

3.4. Optical microscopy

Metallographic investigations were performed by optical microscopy as follows:

A) on unetched samples - for the evaluation of the material inclusions;
B) on etched samples - to highlight the metallographic structure of the steel. The etching was performed with the specific ferrous alloys chemical reagent, Nital 2%. Samples were previously prepared according to standard procedures. Thus, they were cut and, using a coolant in order to avoid local overheating that would modify the structure, they were embedded in resin, ground and polished.

A) Unetched samples

According to standardized principles, the evaluation of the inclusions is made on unetched surfaces at a magnification of 100:1, following the inclusions shape, shade, orientation and distribution.

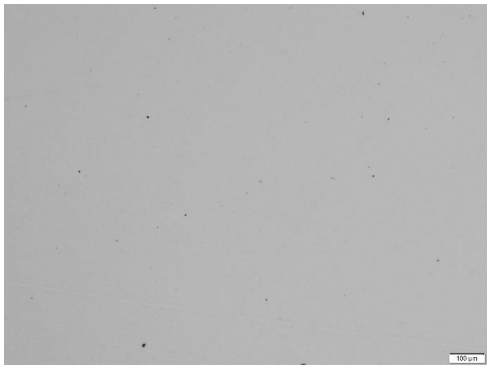
a

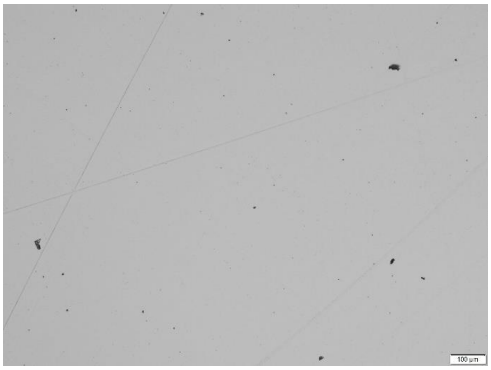
b

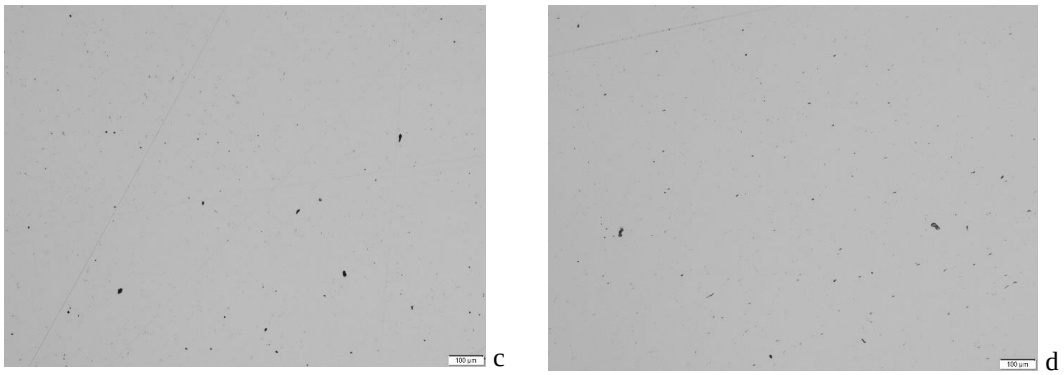

c d

Fig. 6. Optical microscopy of the unetched samples surfaces (a-10, b-11, c-12, d-13)

The samples were studied only in cross section thus the inclusions orientation could not be followed. However, the images are relevant for assessing the inclusions state. Thus, in Figure 6 one can see large, dark brown inclusions, with angular edges specific to alumino-silicates, but also smaller, circular, gray-blue shaded inclusions, belonging to mixed manganese - iron sulfides. Both types of inclusions are endogenous, resulting from the specific smelting - deoxidation reactions that generates oxidic components, such as alumino-silicates and desulphurisation with the formation of mixed manganese - iron sulfides.

The inclusions state of all samples falls within the standardized norms, this being directly dependent on the chemical composition of all four samples, of OLT 45 steel.

B) Etched samples

The microstructures were recorded both at low magnification powers (x100) to provide an overview of the structure, but also at higher magnifications (x500) to observe interesting structural details, revealing features related to the material properties and its operating behavior. The following figures are the optical micrographs of the four analyzed samples.

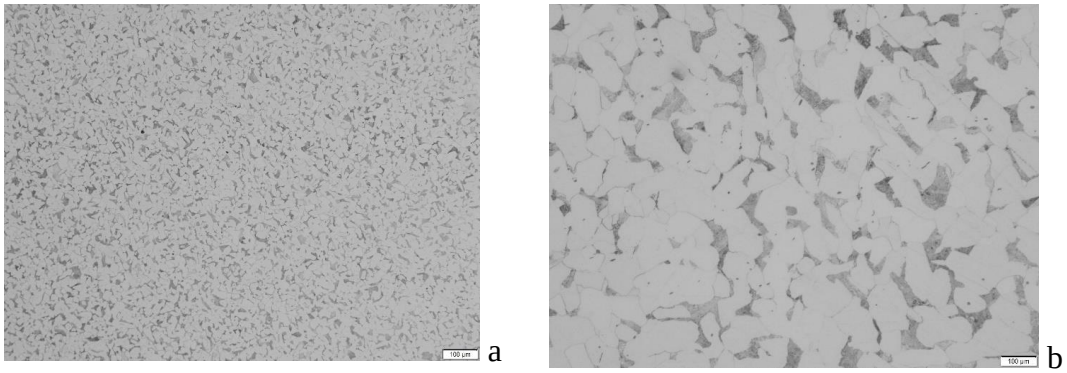

a b

Fig. 7. Optical microscopy micrographs of sample 10, a) M=100x, b) M=500x, reagent Nital 2%

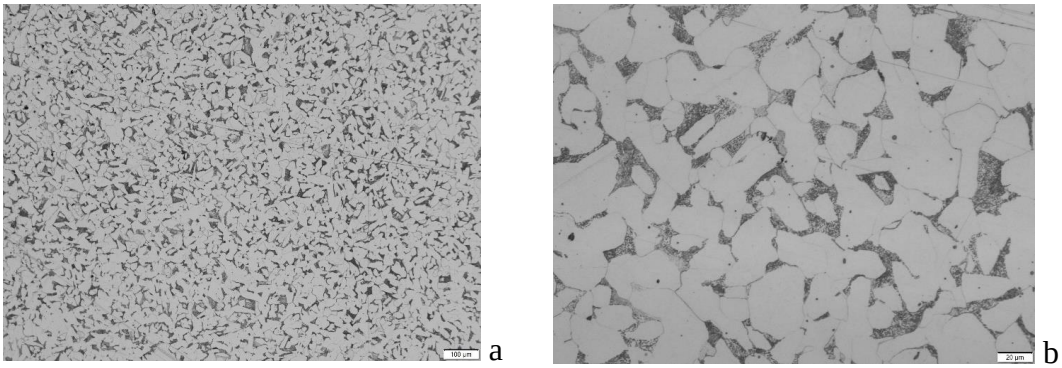
a b

Fig. 8. Optical microscopy micrographs of sample 11, a) M=100x, b) M=500x, reagent Nital 2%

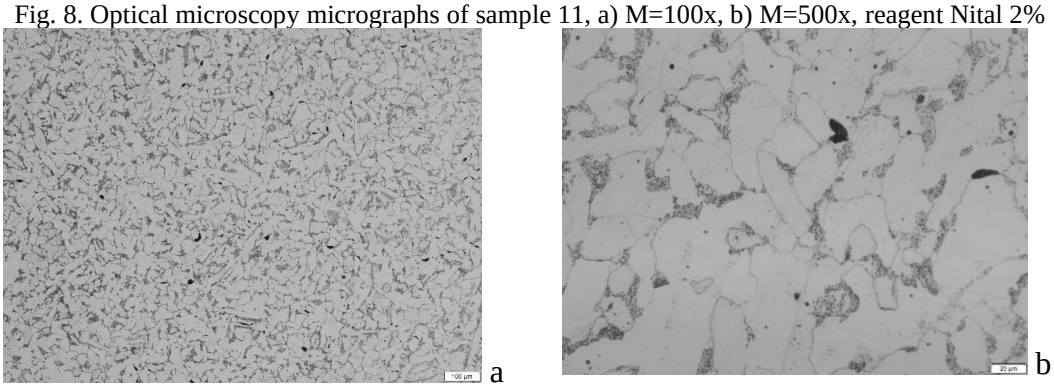
a b

Fig. 9. Optical microscopy micrographs of sample 12, a) M=100x, b) M=500x, reagent Nital 2%

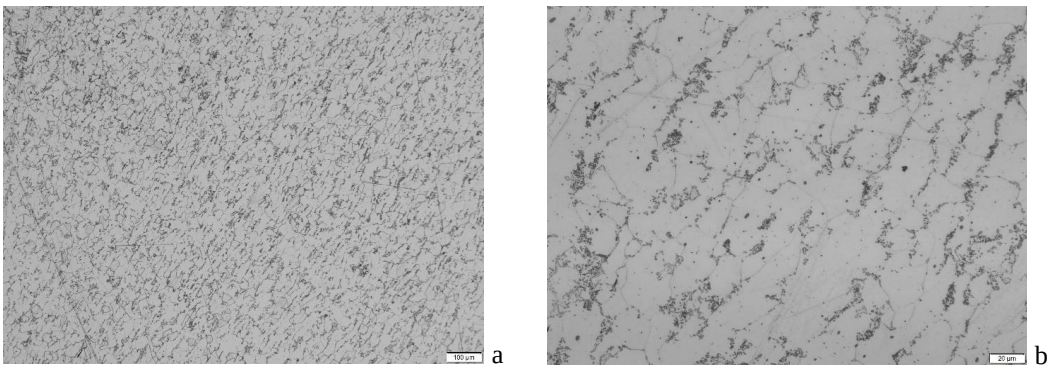
a b

Fig. 10. Optical microscopy micrographs of sample 13, a) M=100x, b) M=500x, reagent Nital 2%

According to theoretical data, a non alloy steel, with a carbon content of about 0.25% as OLT 45 is, has a ferrite-pearlite structure, of about 65% ferrite and 35% lamellar pearlite. These structural details are visible in the four samples analyzed at 100:1 magnification. In addition, the structure is fine (grain size 6-7) which ensures the steel a proper operating behavior.

The metallographic analysis at 500:1 magnification comes with structural interesting informations: in sample 12, lamellar pearlite changes its morphology, acquiring a globular appearance. The spheroidization of pearlite is very evident in sample 13, which was the most strongly degraded by corrosion. One may mention that the spheroidization of pearlite (morphological changes from lamellar to globular) takes place at subcritical temperatures, lower than 728°C. The phenomenon starts at 350 - 400°C, becoming more pronounced as the temperature approaches the critical threshold (728°C). Being based on diffusion phenomena, the process essential parameters are temperature and time; the two are in inverse proportion relationship: the higher the temperature, the higher the transformation kinetics and the shorter the duration; the lower the temperature, the slower the kinetics and the longer the duration.

Concerning the pipes structural analysis, it is not possible to establish precisely their maximum operating temperature, but considering the correct boiler operating parameters, it must have been at the upper limit and the operating time was sufficiently long in order to lead to structural changes. It is important to mention that globular pearlite (with massive spheroidization) induces lower mechanical properties, sometimes necessary in some processing stages. But the pipes are finished products that must not change their properties in operation, so neither the structure. In addition, OLT 45 steel is not part of refractory steels class, consequently the modified structure is an indirect indication that the analyzed pipes have exceeded their service life.

The changes in pearlite morphology from lamellar to globular as the analysis advances towards the most corrosion degraded pipe represents an indirect indication of long operating times at temperatures above 350°C.

From a structural point of view, one may conclude that the pipes (especially pipe 13, the strongly affected by corrosion) have served far beyond their lifespan.

3.5. Scanning electron microscopy (SEM) and EDS chemical analyses

In order to confirm the high temperature operating conditions for the cracked pipes (especially for pipe 13), information can be also brought by studying the iron oxides formed in the corrosion - oxidation area. These data were obtained by scanning electron microscopy investigations associated with energy dispersive analysis spectra.

Two microregions from the corrosion cracking area are presented as follows. Their analysis consists in secondary electrons images of the selected areas, the dispersion of energies spectrum but also the punctual chemical analysis.

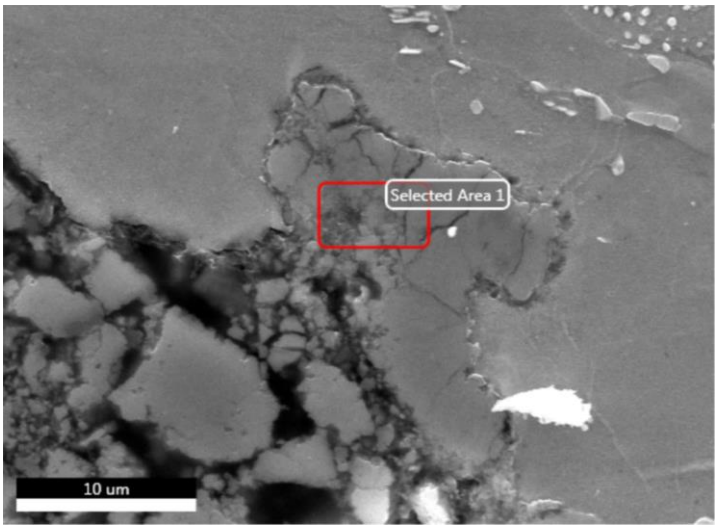

Fig. 11. Secondary electrons image of pipe 13 (Zone 2, Selected Area 1)

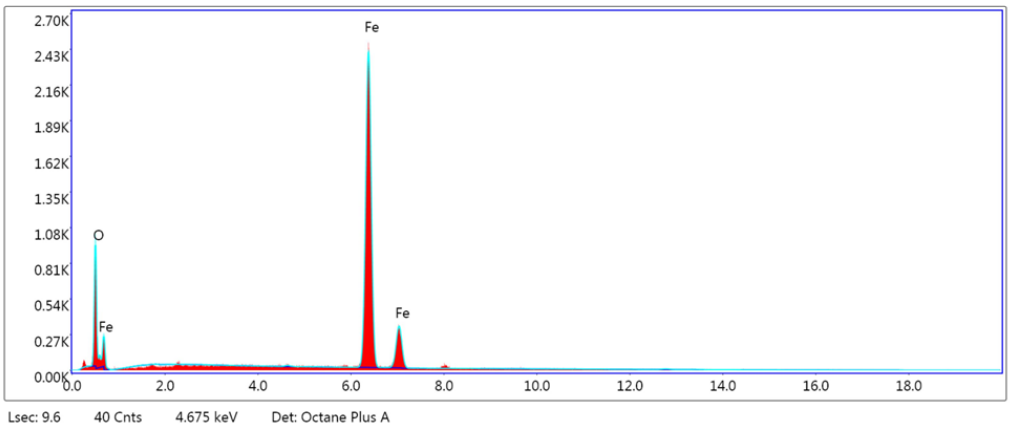

Fig. 12. Energy dispersive spectrum of chemical elements for pipe 13 (Zone 2, Selected Area 1)

Table 4

Local chemical composition for pipe 13 (Zone 2, Selected Area 1)

Element	Weight %	Atomic %	Net Int.	Error %	Kratio	Z	A	F
O K	23.70	52.03	1204.02	7.37	0.1214	1.1624	0.4407	1.0000
FeK	76.30	47.97	7217.03	1.35	0.7259	0.9400	1.0102	1.0020

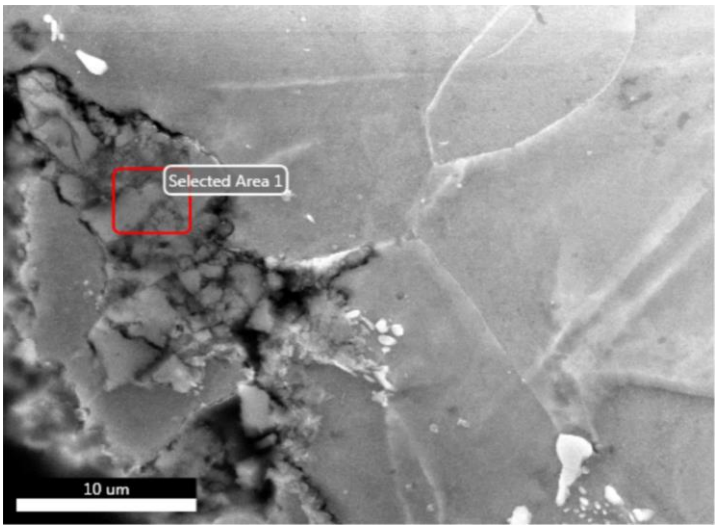

Fig. 13. Secondary electrons image of pipe 13 (Zone 3, Selected Area 1)

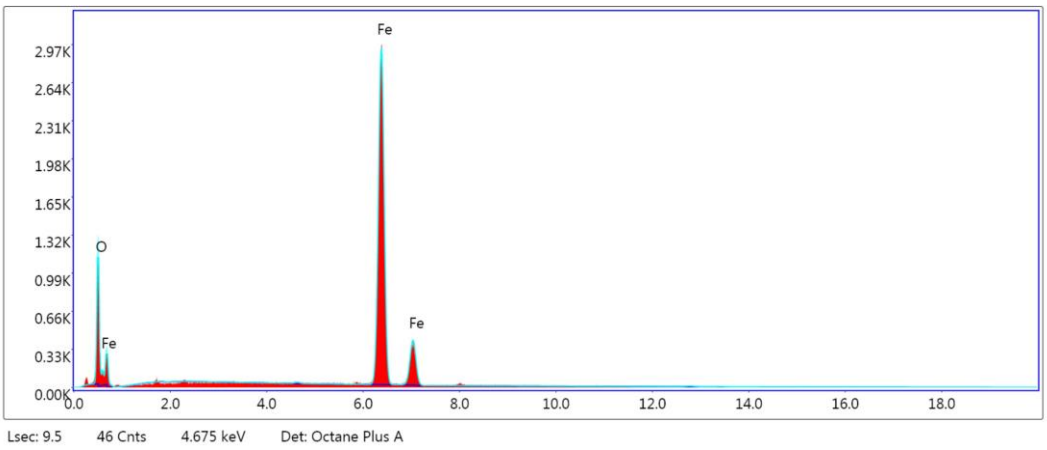

Fig. 14. Energy dispersive spectrum of chemical elements for pipe 13 (Zone 3, Selected Area 1)

Table 5

Local chemical composition for pipe 13 (Zone 3, Selected Area 1)

Element	Weight %	Atomic %	Net Int.	Error %	Kratio	Z	A	F
O K	24.49	53.10	1548.02	7.22	0.1259	1.1602	0.4432	1.0000
FeK	75.51	46.90	8838.76	1.30	0.7172	0.9381	1.0105	1.0021

Fractured microzones are observed in both secondary electron images, their presence resulting in a strong discontinuity of the material. At the same time, the areas are characterized by a certain porosity, which suggests the existence of a high content of iron oxides. The local chemical analysis confirms, through the energy dispersion spectra, the existence of the atomic species Fe and O. In both areas, the local chemical composition is:

- Zone 2, Area 1: 53.03 % at. Fe and 46.93 % at. O
- Zone 3, Area 1: 53.10 % at. Fe and 46.90 % at. O

The atomic percentages of Fe compared to those of O are approximately equal (~ 1: 1) with a slight excess of iron. These data show that the type of iron oxide found is FeO.

According to chemical thermodynamic data [11], ferrous oxide FeO is stable at temperatures above 570°C, which shows that the operating temperature could have reach this much too high value. These results are perfectly in accordance with the optical microscopy studies that shown, according to the structural changes, sufficiently long operating durations at temperatures over 350°C.

3.6. Mechanical tests

The mechanical tests gave the following results for yield strength ($R_{p\ 0.2}$), ultimate tensile strength - resistance to fracture – (R_m) , elongation at break (A %) and striction (Z %):

Table 6

Average values of the tensile test at room temperature (20°C)

No.	Sample	$R_{p\ 0.2}$, MPa	R_m, MPa	A, %	Z, %
1	10	339	502	37	62
2	11	269	424	43	69
3	12	280	438	37	64
4	13	306	507	38	63

Table 7

Average values of the tensile test at high temperature (400°C)

No.	Sample	$R_{p\ 0.2}$, MPa	R_m, MPa	A, %	Z, %
1	10	276	414	32	66
2	11	222	342	50	77
3	12	215	338	56	79
4	13	265	406	43	69

The mechanical characteristics values resulting from the mechanical tests fall within the standard (former STAS 8184 - 87), which regulates the chemical composition and mechanical properties of OLT45 steel.

6. Conclusions

Considering its chemical composition, the metallic material falls into the steel grade OLT 45, frequently used to make pipes from steam boilers. The macroscopic analysis showed an advanced wear, even very strong in some pipes,

due to oxidative corrosion phenomena. The mechanical properties values fall into the right intervals found in OLT 45 steel grade standard.

The metallographic analysis on the unetched surfaces showed a correct inclusion state, in accordance with the steel's standard chemical composition. The metallographic analysis on the etched surfaces highlighted a mostly correct ferritic - pearlitic structure. Some structural details of the pipes that were strongly affected by oxidative corrosion degradation demonstrate that working for long periods of time at high temperatures (over 350°C), led to changes in the pearlite morphology. This fact is a direct information that explains the strong degradation by oxidative corrosion of the pipe labeled with number 13, this assertion being confirmed by scanning electron microscopy and EDS results.

Fractured microzones are observed in both secondary electron images, their presence resulting in a strong discontinuity of the material. The local chemical analysis confirms, through the energy dispersion spectra, the existence of the atomic species Fe and O, the type of iron oxide found being FeO.

Ferrous oxide FeO is stable at temperatures of above 570°C, which shows that the operating temperature could have reach this much too high value. These results are perfectly in accordance with the optical microscopy studies.

The SEM - EDX investigations proved their usefulness by bringing more precise information on the pipes working conditions.

R E F E R E N C E S

[1] *M. Imran*, Effect of Corrosion on Heat Transfer through Boiler Tube and Estimating Overheating, International Journal of Advanced Mechanical Engineering, **vol. 4**, no. 6, 2014, pp. 629-638.

[2] *V. Lazić, D. Arsić, R. Nikolić, D. Rakić, S. Aleksandrović, M. Djordjević, B. Hadzima*, Selection and analysis of material for boiler pipes in a steam plant, International Conference on Manufacturing Engineering and Materials, ICMEM 2016, 6-10 June 2016, Nový Smokovec, Slovakia, in Procedia Engineering, **vol. 149**, 2016, pp. 216 – 223.

[3] *N. Bolt*, High temperature corrosion in modern thermal power generation: gas turbines, high efficiency boilers, IGCC. Journal de Physique IV Proceedings, EDP Sciences, 1993, 03 (C9), pp. C9-741-C9-749

[4] *R. Norling, I. Olefjord*, Erosion-corrosion of Fe- and Ni-based alloys at 550°C, Wear, vol. 254, 2003, pp. 173-184.

[5] *R. A. Rapp*, Chemistry and electrochemistry of hot corrosion of metals, Mater. Sci. Eng., vol. 87, March 1987, pp. 319-327.

[6] *J. Stringer*, High temperature corrosion problems in coal based power plant and possible solutions, Proceedings of International Conference on Corrosion 'CONCORN' 97, December 3-6, 1997, Mumbai, India, pp 13-23.

[7] *G. Bakić, V. Šijački Žeravčić, M. Đukić, B. Anđelić*, Probability of Failure of Thermal Power Plant Boiler Tubing System Due to Corrosion, FME Transactions, **vol. 35**, 2007, pp. 47-54.

[8] *Y. Xie, J. Zhang*, Corrosion and deposition on the secondary circuit of steam generators, Journal of Nuclear Science and Technology, **vol. 53**, no. 10, 2016, pp. 1455-1466.

[9] *G. Yang, Y. Gou, X. Liu, X. Zhang, T. Zhang*, Failure Analysis of the Corroded Water Wall Tube in a 50 MW Thermal Power Plant, High Temp. Mater. Proc., **vol. 37**, no. 9-10, 2018, pp. 995–999.

[10] *Y. Li, C. Liu, F. He, F. Wang*, Analysis on Water Wall Tube Explosion in a Power Plant, 2nd International Conference on Advances in Civil Engineering, Energy Resources and Environment Engineering May 22-24, 2020, Nanning, China, IOP Conf. Series: Earth and Environmental Science, **vol. 526**, 2020, 012162.

[11] *T. Dulămiţă, E. Florian*, Tratamente termice şi termochimice (Heat Treatments and Thermochemical Treatments), Editura Didactică şi Pedagogică, Bucureşti, 1982.